Biological Nanofactories Target and Activate Epithelial Cell Surfaces for Modulating Bacterial Quorum Sensing and Interspecies Signaling

Colin G. Hebert,[†,⊥] Apoorv Gupta,[§] Rohan Fernandes,[†,⊥] Chen-Yu Tsao,[†,⊥] James J. Valdes,[‡] and William E. Bentley[†,§,⊥,*]

[†]Center for Biosystems Research, University of Maryland Biotechnology Institute, 5115 Plant Science Building, College Park, Maryland 20742, United States, [‡]U.S. Army Edgewood Chemical Biological Center, AMSRD-ECB-AP-B/Michel E3330, 5183 Black Hawk RD, Aberdeen Proving Ground, Maryland 21010, United States, [§]Department of Chemical and Biomolecular Engineering, University of Maryland College Park, College Park, Maryland 20742, United States, and [⊥]Fischell Department of Bioengineering, Room 2330 Jeong H. Kim Engineering Building (Bldg. #225), University of Maryland College Park, College Park, Maryland 20742, United States

ABSTRACT In order to control the behavior of bacteria present at the surface of human epithelial cells, we have created a biological "nanofactory" construct that "coats" the epithelial cells and "activates" the surface to produce the bacterial quorum sensing signaling molecule, autoinducer-2 (AI-2). Specifically, we demonstrate directed modulation of signaling among *Escherichia coli* cells grown over the surface of human epithelial (Caco-2) cells through site-directed attachment of biological nanofactories. These "factories" comprise a fusion protein expressed and purified from *E. coli* containing two AI-2 bacterial synthases (Pfs and LuxS), a protein G IgG binding domain, and affinity ligands for purification. The final factory is fabricated *ex vivo* by incubating with an anti-CD26 antibody that binds the fusion protein and specifically targets the CD26 dipeptidyl peptidase found on the outer surface of Caco-2 cells. This is the first report of the intentional "*in vitro*" synthesis of bacterial autoinducers at the surface of epithelial cells for the redirection of quorum sensing behaviors of bacteria. We envision tools such as this will be useful for interrogating, interpreting, and disrupting signaling events associated with the microbiome localized in human intestine and other environments.

KEYWORDS: quorum sensing · bacterial signaling · *Escherichia coli* · Caco-2 · nanofactories · autoinducer-2

Eukaryotic cell to cell communication and signaling pathways have long been known to influence a wide variety of biological processes, including gene expression,[1] cell death,[2,3] and differentiation.[4,5] Although initially less well-known, certain bacterial species also use small signaling molecules in order to communicate and coordinate multicellular behavior. Termed quorum sensing (QS),[6] the transduction of biological signals has been linked to numerous bacterial behaviors including bioluminescence,[7,8] pathogenicity,[9,10] biofilm formation,[11,12] and other diverse phenotypes.[13,14] Since many of these behaviors are undesirable from a human health perspective, molecules that can inhibit or modulate bacterial communication have been proposed as a next-generation treatment for bacterial infections.[15] Additionally, several human diseases are directly or indirectly linked to the population of microorganisms that colonizes the gastrointestinal tract. A recent review summarizing the interplay between mammalian and bacterial signal molecules (interkingdom signaling) further underscores the importance of understanding the nature of these interactions.[16] Tools that enable the interrogation and modulation of bacterial signaling will advance our understanding of the bacteria−bacteria and bacteria−human cell interactions. The directed placement of signal molecules at specific sites is one example.

Targeted delivery is one of the most important and challenging aspects of any molecular therapy. Most approaches focus on pairing the effector molecule with a suitable carrier, either through conjugation or encapsulation. These carriers can include microspheres,[17,18] nanoparticles,[19−21] and liposomes.[22,23] Recently, we implemented an approach originally conceptualized by LeDuc *et al.*,[24] in which effector molecules are synthesized from locally available precursors directly on cell surfaces through the use of biological nanofactories.[25] The conceptual nanofactory consists of several functional units or modules, each of which can be composed of several different molecules or subassemblies that must be appropriately assembled for a functional unit. These modules can target a specific area or type of cells (targeting), sense and transport

*Address correspondence to bentley@eng.umd.edu.

Received for review June 10, 2010 and accepted October 15, 2010.

Published online October 28, 2010.
10.1021/nn1013066

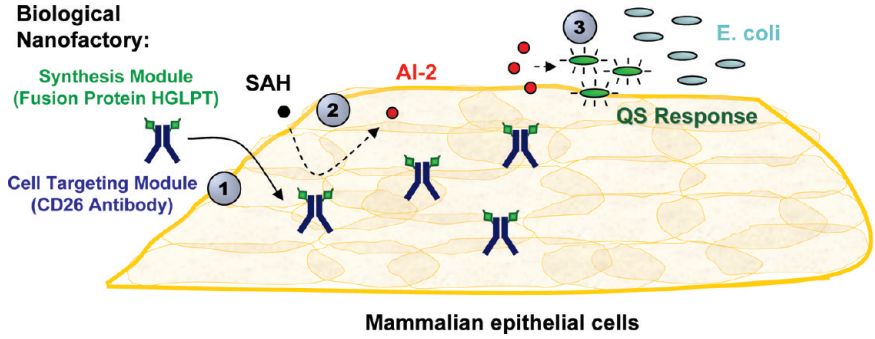

Figure 1. Altering bacterial response through cell-surface targeted autoinducer 2 (AI-2) synthesis. The biological nanofactory is composed of the synthesis element (fusion protein HGLPT) and the targeting element (CD26 antibody). (1) Nanofactory binding to the surface of Caco-2 mammalian epithelial cells is mediated by the CD26 antibody. (2) Once bound, the substrate *S*-adenosyl homocysteine (SAH) is added and processed to AI-2 by the synthesis element of the nanofactory. (3) Signaling molecule AI-2 is detected by the *E. coli* present near the Caco-2 cells, eliciting a quorum sensing response.

available substrates (sensing), synthesize effector molecules (biosynthesis), and self-destruct upon completion (self-destruct).[24] The previously reported nanofactories contained a novel fabrication domain that facilitated flexible self-assembly of the functional units; they were able to trigger a bacterial response in the absence of native bacterial signals as well as elicit a targeted response in a specific species within a mixed bacterial culture.[26]

Here, we present the first interkingdom application of biological nanofactories for the modulation of the QS response in bacteria grown in co-culture with human epithelial cells (Figure 1). The constructs are composed of three functional modules: the cell targeting module, the fabrication module, and the synthesis module. The cell targeting module is composed of an antibody raised against the human CD26 protein, a GLP1 peptidase, which facilitates targeting the surface of Caco-2 mammalian epithelial cells (ATCC CRL-2102). The fabrication module is an IgG binding domain expressed in *E. coli* as a fusion protein with the synthesis module. The synthesis module, in turn, consists of the fusion protein HGLPT developed previously[26] that can synthesize the "universal" bacterial signaling molecule autoinducer-2 (AI-2; recognized by over 70 bacterial species[27,28]). AI-2-based signaling influences a number of bacterial behaviors, including biofilm formation in *E. coli*,[29,30] luminescence and type III secretion of virulence factors in *Vibrio harveyi*,[31,32] and the commensal biofilm formation of the oral bacteria *Actinomyces naeslundii* and *Streptococcus oralis*.[33]

Thus, given the wide ranging effects and complex nature of signaling among bacteria and their hosts,[16] the ability to target the synthesis of AI-2 to a specific location could prove a valuable tool for studying these interactions. We hypothesized that the assembly of these structures and their targeting to a specific location—the surface of Caco-2 cells—could create a "bioactive" surface with the ability to synthesize AI-2 using locally available substrates, thereby signaling bacterial cells near the epithelial surface and affecting their behavior. By directing their behavior in a specific manner, the bacteria could become less harmful or even serve a beneficial purpose. This targeted synthesis could allow for a localized high concentration of the signaling molecule at the epithelial cell surface, something that would be difficult to achieve using bulk delivery of AI-2.

Our concept is depicted in Figure 1. When added to a monolayer of Caco-2 cells, the nanofactories attach to the cell surface (Figure 1, step 1), where they can synthesize AI-2 from the available substrate *S*-adenosyl homocysteine (SAH, Figure 1, step 2). *E. coli* bacteria that have been added to the culture can then sense and respond to the AI-2, resulting in a quorum sensing response (Figure 1, step 3). Our results demonstrate successful altering of the bacterial quorum sensing response as a result of small molecule synthesis enabled by the nanofactory attached to the surface of mammalian epithelial cells.

RESULTS AND DISCUSSION

Assembly and Targeting the Biological Nanofactory. The biological nanofactories used in this study are composed of two main elements. The targeting element is a monoclonal antibody raised against the human CD26 protein (Santa Cruz Biotech, sc-19607), which is a membrane glycoprotein and serine exopeptidase.[34] CD26 was selected from among several candidates due to its reported high expression (98%) on the surface of Caco-2 cells.[35] A phycoerythrin (PE)-labeled CD26 antibody was used to qualitatively and quantitatively assess its suitability for targeting the nanofactory to the cell surface (Figure S1 in Supporting Information). Confocal images (Figure S1A,B) show binding of the CD26 antibody to the surface of Caco-2 cells counterstained with 4′,6-diamidino-2-phenylindole (DAPI). The images indicate that the CD26 antibody binds to the membrane surface of the cells, which is the desired location, as it facilitates non-invasive binding of the antibody and easy access for the substrate. Binding of the CD26 antibody was quantitatively analyzed using flow cytometry (Fig-

ure S1C,D). Prior to analysis, cells were harvested using 0.2% EDTA in order to preserve their surface features and incubated with the labeled antibody for 30 min before washing and subsequent fixation with 4% paraformaldehyde (PFA). Analysis shows that 90 ± 3% (standard deviation) of the Caco-2 cells present enough CD26 protein on their surface to be detected using flow cytometry. This high percentage of expression coupled with the location of binding made CD26 a promising choice as the targeting domain.

The biosynthesis component in this study is the 57 kDa fusion protein HGLPT (HGLPT: His_6-protein G-LuxS-Pfs-Tyr_5).[26] HGLPT facilitates antibody binding through protein G[36,37] and can synthesize the bacterial quorum sensing molecule AI-2 from the substrate SAH in a two-step process using the enzymes Pfs and LuxS.[38−41] Thus, HGLPT contains both a synthesis domain and a fabrication domain, which allows for facile self-assembly. Nanofactories composed of CD26 antibody (5 μg/mL) and HGLPT (5 μg/mL, 0.09 μM) were assembled by mixing the two components in PBS buffer +1% BSA (PBS-BSA) before adding them to the Caco-2 cells. In order to visualize binding to the cell surface, HGLPT was labeled using Alexa Fluor 488. As shown in Figure 2, cells treated with both anti-CD26 and HGLPT (nanofactories) and subsequently stained with DAPI (Figure 2B) show a greater level of green fluorescence than cells treated with only HGLPT (Figure 2A). This indicates that the binding to the cell surface is mediated by the CD26 antibody and that the HGLPT binds to the CD26 antibody, resulting in effective targeting to the Caco-2 cell surface. Flow cytometry was again used to quantify the HGLPT and nanofactory binding, using Alexa Fluor 647 labeled HGLPT. While a small percentage of cells (14 ± 1.4%) shows fluorescence as a result of the nonspecific binding of HGLPT, the vast majority (83 ± 3.6%) of cells treated with both anti-CD26 and HGLPT show strong fluorescence (for histograms, see Supporting Information Figure S2). Since ~90% of the cells express CD26 (Figure S1D), this demonstrates that just over 90% of those cells can be targeted using these constructs.

Cell-Surface Autoinducer-2 Synthesis. After successfully targeting the surface of Caco-2 cells, studies were conducted to measure the AI-2 synthesis capabilities of the nanofactories. To do this, a confluent layer of Caco-2 cells in a 24-well plate was incubated with either HGLPT (25 ug/mL) or anti-CD26 and HGLPT (10 μg/mL CD26, 25 μg/mL HGLPT) for 30 min at 37 °C, washed three times with PBS-BSA to remove nonspecifically bound HGLPT, and incubated with a solution of 1 mM SAH in DMEM containing no glucose. At various time points, the medium was removed from the cells and stored at −20 C until further analysis. AI-2 activity of the medium was quantified using the *V. harveyi* BB170 reporter strain, which luminesces in response to AI-2 present in the culture medium.[42] On the basis of time course data (Figure S3A), it was determined that a 2 h synthesis period is sufficient to elicit a strong quorum sensing response from BB170, while little to no response was detected in cell-free medium from Caco-2 monolayers incubated with only HGLPT. Additional controls of untreated cells, SAH only, and HGLPT only (no SAH) were tested, none of which elicited an AI-2-based response from BB170 (data not shown). As shown in Figure 3, additional experiments were conducted using varying amounts of HGLPT (from 2−25 μg/mL, 500 μM SAH) or incubated in different concentrations of SAH (from

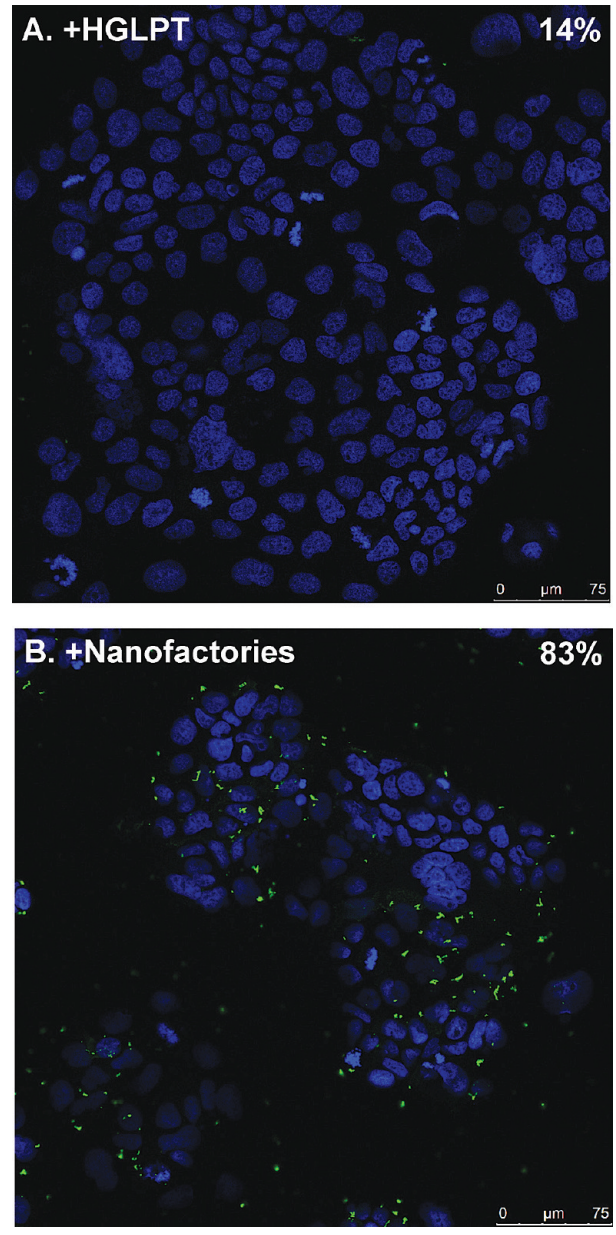

Figure 2. Targeting the biological nanofactory to the surface of Caco-2 cells. Confocal images taken of Caco-2 cells stained with DAPI + Alexa Fluor 488 HGLPT (A) or DAPI + biological nanofactories (AF 488 HGLPT + unlabeled CD26 antibody) (B). Cells were fixed with 4% paraformaldehyde and mounted with Prolong Gold. Magnification is 400×. The percentage on each graph indicates the average percentage of cells with a detectable level of fluorescence (and thus targeted by the nanofactory), as measured by flow cytometry.

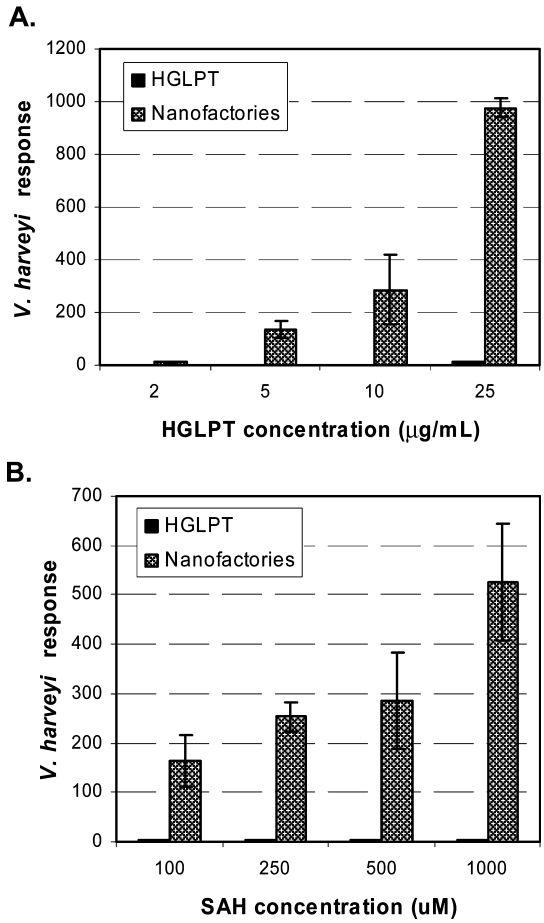

Figure 3. Cell-surface targeted AI-2 synthesis: *V. harveyi* response. *V. harveyi* BB170 quorum sensing response after incubation with medium from Caco-2 cells plus either HGLPT only (concentrations as indicated) or nanofactories (CD26 antibody 10 μg/mL). (A) BB170 response with varying concentrations of HGLPT (500 mM SAH) and (B) BB170 response with varying concentrations of SAH (HGLPT 10 μg/mL). Error bars represent standard error of the mean.

100 to 1000 μM, 10 μg/mL SAH). In both cases, the AI-2-based response decreases with decreasing amounts of SAH or HGLPT, while the amount of response from cells incubated with only HGLPT is far lower. It was also possible to carry out several independent 2 h synthesis periods using the same activated monolayer of Caco-2 cells (Figure S3B). The first two synthesis periods show nearly the same amount of QS response, while the third and fourth periods show a decreased response (75 and 40%, respectively). By comparison, this response is still over 25 times greater than the nonspecific response as a result of the HGLPT only control.

To further investigate the AI-2 production capabilities of these constructs, an AI-2 responsive strain of *E. coli*, MDAI2 (pCT6+pEGFPuv), was used. Developed previously,[43] this autoinducible system uses two plasmids. The first contains elements from the *E. coli* quorum sensing system and drives T7 RNA polymerase expression in response to AI-2. The second is a commercially available vector containing T7 RNA polymerase-driven GFP. Thus, these cells produce GFP

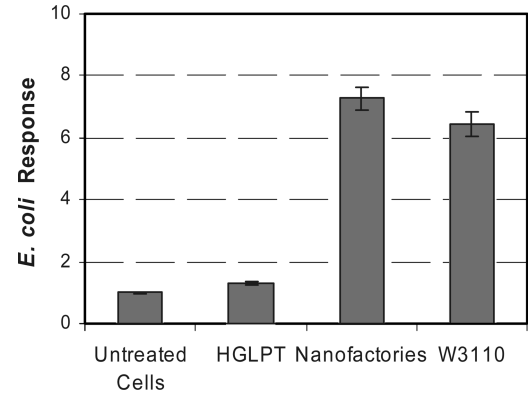

Figure 4. Cell-surface targeted AI-2 synthesis: *E. coli* response. *E. coli* MDAI2 (pCT6+pEGFPuv) quorum sensing response after incubation with medium from Caco-2 cells plus PBS buffer (Untreated Cells), HGLPT only (25 μg/mL), or nanofactories (CD26 10 μg/mL, HGLPT 25 μg/mL). *E. coli* W3110 (pCT6+pEGFPuv) cells were treated with only PBS buffer. *E. coli* response is presented as the change in fluorescence over the 12 h incubation period, normalized to the fluorescence change of untreated cells (Δfluorescence for untreated cells = 1). Error bars represent standard error of the mean.

in response to AI-2. Further, since they do not produce their own AI-2,[44] they can serve as a reporter strain to assess the QS response in *E. coli*.

In order to test the response of MDAI2 (pCT6+pEGFPuv), anti-CD26 and HGLPT were added to a monolayer of Caco-2 cells ("Nanofactories"), which was then washed three times with PBS-BSA and incubated with a 1 mM solution of SAH in PBS for 2 h, at which point the medium was removed and stored at −20 °C or used directly for analysis. PBS buffer was used in this and subsequent experiments in order to avoid any repression of the AI-2 response as a result of catabolite repression by glucose and other sugars through the cyclic AMP-CRP complex.[45] Additional controls included untreated Caco-2 cells ("Untreated Cells") as well as cells to which only HGLPT was added ("HGLPT"). For analysis, 200 μL of the cell-free fluid samples from all three groups was aliquoted into a black-walled clear-bottom 96-well plate. A sufficient volume of MDAI2 (pCT6+pEGFPuv) *E. coli* growing in the exponential phase (OD 0.4−0.5) was then added to the wells in order to give a final starting OD of 0.025. Another strain of *E. coli*, W3110 (pCT6+pEGFPuv), which can produce its own AI-2, was also analyzed as a positive control. Anti-CD26 and HGLPT were not added to this control. Thus, any AI-2-based response would be a result of native AI-2 synthesis. The cells were then grown at 37 °C in the plates for a 12 h period, throughout which their GFP expression was monitored (Figure 4). Cells incubated with media from the "Untreated Cells" group show very little increase in fluorescence over the incubation period, while cells incubated with samples from "HGLPT Only" show just 30% more fluorescence than untreated cells. However, cells incubated with medium from the "Nanofactories" group show a strong increase in fluo-

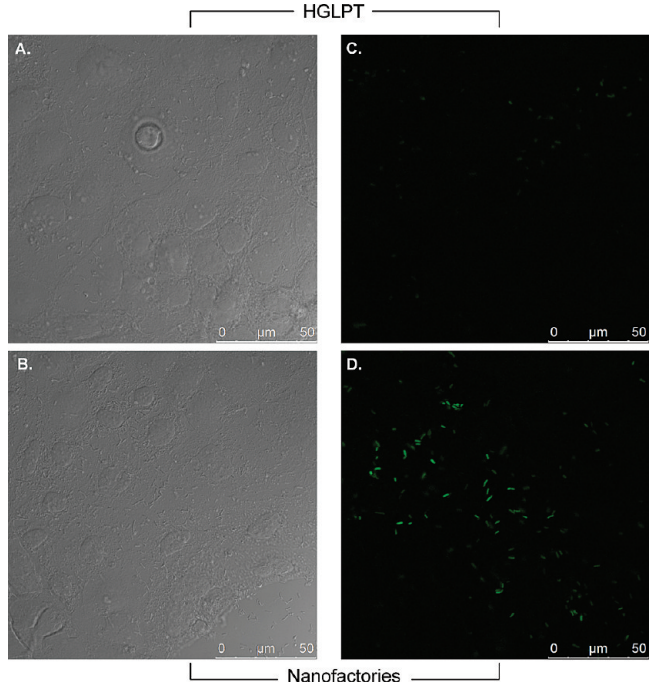

Figure 5. Modulating quorum sensing response in Caco-2/*E. coli* co-cultures. Confocal DIC and fluorescent images of co-cultures of Caco-2 cells with MDAI-2 (pCT+pEGPuv) *E. coli* and either HGLPT (A,C) or biological nanofactories (B,D). (A,B) DIC channel showing *E. coli* on the surface of Caco-2 cells. (C,D) Fluorescent channel showing GFP expression in *E. coli*. Cells were fixed with PFA and mounted with Prolong Gold prior to imaging. Magnification is 630×.

rescence, which is over 7 times that of medium from untreated cells and 5.5 times that of medium from HGLPT only cells. The fluorescence from this group of cells is also slightly higher than the wild-type response from W3110 cells that were not exposed to any exogenously produced AI-2, though this difference is not statistically significant ($p > 0.05$, *t* test). This large increase in fluorescence shows that MDAI2 (pCT6+pEGFP) *E. coli* cells can sense and respond to the AI-2 produced by the nanofactories at the Caco-2 cell surface and that the level of response is similar to that seen in wild-type cells. Also, the minimal response as a result of nonspecifically bound HGLPT shows that the AI-2 synthesis has been effectively targeted to the Caco-2 cell surface using the CD26 antibody.

Stimulating a Quorum Sensing Response in Co-cultures. Once it was apparent that biologically active AI-2 could be synthesized, the next step was the investigation of *E. coli* and Caco-2 cell co-cultures. Such co-cultures have been used in the past to simulate the environment of the gut.[46,47] Thus, the ability to manipulate bacteria in a co-culture could provide additional insight into the interaction between bacteria and their hosts studied in these simulations. As in previous experiments, Caco-2 cells were grown for 72 h on coverslips prior to treatment with either anti-CD26 + HGLPT or HGLPT. After a 2 h synthesis period, exponential phase MDAI2 (pCT6+pEGFPuv) cells were added to a final OD of 0.01 in a solution of 1 mM SAH in PBS. Following an overnight incubation period (approximately 15 h), cells were fixed and mounted on glass slides for visualization using confocal microscopy. Results are presented in Figure 5. Differential interference contrast images (Figure 5A,B) show *E. coli* on the surface of Caco-2 cells treated with both HGLPT and nanofactories. However, when looking at GFP fluorescence (Figure 5C,D), only Caco-2 cells to which both anti-CD26 and HGLPT were added are able to elicit an AI-2-based response (GFP production) in *E. coli*. This demonstrates cell-surface targeted production of a quantity of AI-2 sufficient to elicit a quorum sensing response in *E. coli* present at the cell surface.

Modulating Native Bacterial Signaling Using Targeted Small Molecule Synthesis. Since many species of bacteria (including *E. coli*) that participate in quorum sensing both produce and respond to autoinducers, one potential application of these biological nanofactories would be the modulation of *native* bacterial communication. This would enable the cell-surface targeted production of AI-2 to potentially affect a phenotypic change in the neighboring species of bacteria. In order to demonstrate this concept, co-culture experiments were conducted with nanofactories attached to Caco-2 cells and W3110 (pCT6+pEGFPuv) *E. coli*, a strain that produces GFP in response to AI-2 and retains the native ability to synthesize its own AI-2. After a 2 h synthesis period, aliquots of exponentially growing *E. coli* were added to Caco-2 cell monolayers treated with either anti-CD26 + HGLPT (nanofactories), HGLPT, or PBS-BSA only (untreated cells) to a final OD of 0.01 in PBS + 1 mM SAH. At various time points (Figure 6), *E. coli* cells were removed from the cultures and analyzed using flow cy-

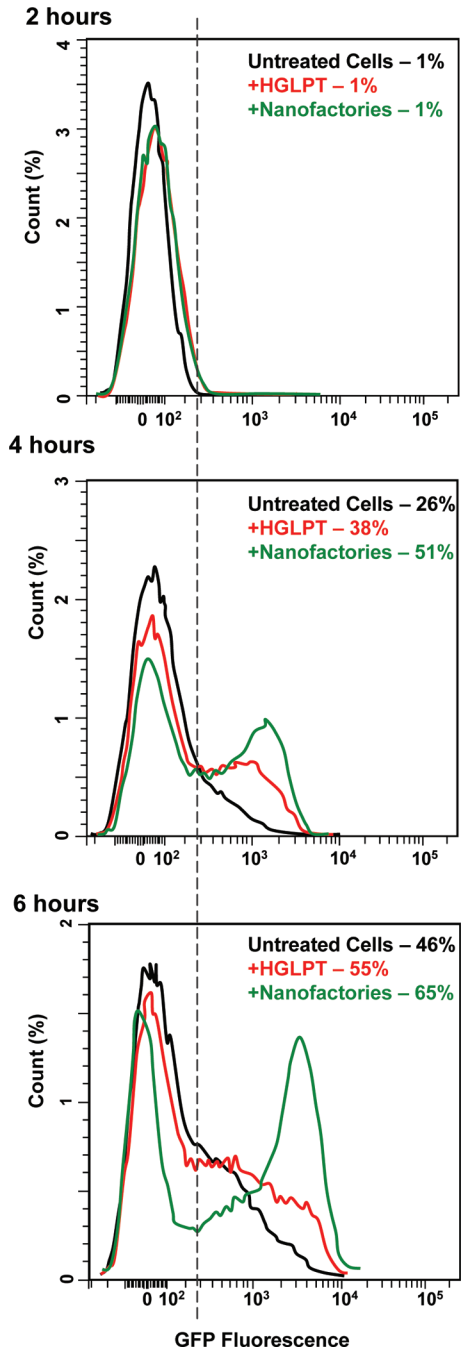

Figure 6. Increasing the native quorum sensing response in *E. coli*. Flow cytometry histograms representing the GFP fluorescence of *E. coli* W3110 (pCT6+pEGFPuv) cells that had been co-cultured with Caco-2 cells for 2, 4, and 6 h. The Caco-2 cells had been previously treated with PBS (Untreated Cells), HGLPT only (HGLPT, 25 μg/mL), or biological nanofactories (CD26 10 μg/mL, HGLPT 25 μg/mL) and incubated with PBS + 1 mM SAH for 2 h prior to the addition of the *E. coli*.

tometry. After 2 h, almost no fluorescence can be seen in any of the groups. However, at 4 and 6 h, there is a considerable amount of fluorescence in all three groups, demonstrating that the cells are responding to AI-2. At both time points, the highest percentage of fluorescent cells is present in the nanofactories group (51% at 4 h, 65% at 6 h), followed by HGLPT (38 and 55%) and untreated cells (26 and 46%). Moreover, the average fluorescence was also highest in the nanofactories group, especially at the 6 h time points (~3000 versus ~2000 and ~1400 for HGLPT and untreated cells, respectively). Thus, the cell-surface targeted production of AI-2 was able elicit a significantly ($p < 0.01$, $n = 5$) higher percentage of fluorescent cells and average fluorescence than the native signaling alone. That is, the cells tested in this experiment made their own functional AI-2 (hence positive response in control experiments), but the addition of the nanofactories at the surface of the Caco-2 cells provided an additional source of AI-2 which was transported to the nearby cells, resulting in modulated behavior. This demonstrates that the production of AI-2 from the nanofactories can *enhance* the native quorum sensing response of wild-type bacteria.

CONCLUSION

A number of potential applications exist for these or similarly designed constructs as aids in research or as practical treatments. Eliciting a quorum sensing response at a lower than typical cell density might prove to be a useful research tool for the study of quorum sensing or as a biosensor for detection of potentially harmful bacteria. Such a sensor could detect harmful bacteria before they become virulent or organize into a biofilm, allowing for easier treatment. It is also possible that cell-surface targeted production of a signaling molecule could interfere with the quorum sensing response in such a way as to reduce virulence. Such an application has already been demonstrated in *Vibrio cholerae* cells by overproducing cholera autoinducer 1 (CA-1) with *E. coli*.[46,48] Other bacterial and mammalian signaling molecules, such as epinephrine, norepinephrine, and indole, have been shown to affect the expression of certain virulence-related genes in *E. coli* O157:H7 (EHEC).[30,49] The presence of indole, in particular, has been shown to attenuate the motility, biofilm formation, and attachment of EHEC cells.[30] Since the gastrointestinal tract contains an estimated 10^{14} bacteria comprising hundreds of species[50] engaged in a complex signaling network among themselves and human epithelia,[51−53] any number of applications could be envisioned for engineered biological nanofactories with the ability to produce specific effector molecules either to initiate or to respond to specific events or signals within the GI tract.

MATERIALS AND METHODS

Epithelial Cell Culture. Caco-2 clone C2BBe1 epithelial cells (ATCC# CRL-2102) were maintained in Dulbecco's modified Eagle media (Invitrogen, 10566-016) plus 10% FBS (Sigma, F0926) and 0.01 mg/mL human transferrin (Sigma, T8158) at 37 °C in a humidified incubator supplemented with 5% CO_2. Cells were passaged every 3−4 days at 80−90% confluence. Unless otherwise noted, all experiments were conducted in 24-well plates seeded

at a density of 250 000 cells/mL (125 000 cells/well) and experiments were started 72 h post-seeding.

Bacterial Strains and Growth Conditions. All *E. coli* strains were cultured in Luria−Bertani (LB) medium at either 30 or 37 °C with vigorous shaking (250 rpm) unless otherwise noted. The LB medium used for bacterial growth contained 5 g/L of yeast extract (Sigma Aldrich, St. Louis, MO), 10 g/L of Bacto tryptone (Difco) and 10 g/L NaCl (J.T. Baker). Media were supplemented as necessary by antibiotics (either ampicillin or kanymycin) at a concentration of 50 μg/mL, unless otherwise noted.

Expression and Purification of HGLPT. The fusion protein HGLPT was expressed and purified as described previously.[26] Briefly, *E. coli* BL21 luxS-pHGLPT[26] was cultured at 37 °C and 250 rpm in LB medium supplemented with 50 μg/mL ampicillin. When the optical density (OD 600 nm) of the cell culture was between 0.4 and 0.6, 1 mM IPTG was added to induce overexpression of HGLPT. After a 6 h induction period at the same culture conditions, cells were harvested by centrifugation at 12 000*g* for 15 min at 4 °C. The cell pellet was either stored at −20 °C or resuspended directly into PBS buffer (pH 7.2) + 10 mM imidazole. The resuspended cells were then lysed by sonication using a sonic dismembrator 550 (Fisher Scientific). The soluble cell extract was collected by centrifugation at 14 000*g* for 15 min at 4 °C, filtered through a 0.22 μm polyether sulfone, low protein binding filter (Millipore), and then loaded on a pre-equilibrated immobilized metal-ion affinity chromatography (IMAC) column (HiTrap Chelating HP, GE Healthcare Life Sciences). After two wash steps (wash 1:20 mM PO_4^{3-}, 250 mM NaCl, and 10 mM imidazole; wash 2:20 mM PO_4^{3-}, 250 mM NaCl, and 50 mM imidazole), HGLPT was eluted with 20 mM PO_4^{3-}, 250 mM NaCl, and 350 mM imidazole. The protein was then desalted using an Amicon Ultra-15 centrifugal unit (NMWL 10000; Millipore), resuspended in PBS buffer, and stored at −80 °C until use.

Protein Labeling. Purified HGLPT was labeled with either Alexa Fluor 488 (Invitrogen, A10235) or Alexa Fluor 647 (A20173) per the manufacturer's recommendation. Briefly, 2 mg of protein was reacted with the labeling solution for 1 h at room temperature and then purified using the column included in the labeling kit. Once the labeled protein was separated from the unconjugated dye, its concentration was measured and the degree of labeling was determined.

Nanofactory Assembly and Attachment to Caco-2 Cells. The biological nanofactories were composed of two elements: the fusion protein HGLPT (either labeled or unlabeled) and a mouse monoclonal antibody raised against the human CD26 protein (Santa Cruz Biotech, sc-19607). Nanofactories were assembled by mixing the CD26 antibody (10 μg/mL unless otherwise noted) with HGLPT (various concentrations) in PBS + 1% BSA (PBS-BSA). Two hundred microliters of the nanofactory (or control) solution was then added to a confluent layer of Caco-2 cells (72 h post-seeding) that had been previously washed once with 500 μL of PBS. Control solutions included PBS-BSA only, as well as PBS-BSA + HLPGT (no antibody). After addition, solutions were incubated with the Caco-2 cells at 37 °C for 30 min, followed by three washes with PBS-BSA. Then a solution of 1 mM SAH in either PBS buffer or DMEM no glucose (Invitrogen 11966-025) was added to the cells and incubated for the indicated length of time. Upon completion of the AI-2 synthesis, the medium was removed from the wells and stored at −20 °C until analysis.

Immunofluorescence and Confocal Imaging. All images were taken on a Leica SP5 X confocal microscope. In order to prepare samples for imaging, Caco-2 cells were seeded on 12 mm glass coverslips (Fisher, NC9708845) that had been sterilized and placed within 24-well plates. Once the cells had reached confluence (approximately 72 h post-seeding), the medium was removed from the well and the cells were washed once with PBS. Then, 500 μL of ice cold 4% paraformaldehyde in PBS was added to the wells for 15 min at room temperature. Following fixation, the cells were washed three times with 500 μL of PBS-BSA. Then, 200 μL of either the phycoerythrin (PE)-labeled antibody solution (5 μg/mL), nanofactories constructed with Alexa 488 labeled HGLPT (5 μg/mL unlabeled antibody, 7 μg/mL HGLPT), or various control solutions were added to the wells and incubated on ice for 30 min. After another three washes with PBS-BSA, a 3 μM solution of DAPI (Invitrogen, D1306) in PBS was added to the cells for 5 min, followed by a final three washes with PBS. Finally, the PBS was aspirated from the well, and the coverslip was removed, dried, and mounted onto a glass slide using Prolong Gold Antifade Reagent (Invitrogen, P36930). Control and experimental images were taken under identical conditions using the Leica Application Suite Advanced Fluorescence software package and exported as TIF files for presentation without further modification. DAPI was imaged using a 405 nm UV diode label and an emission of 414−478 nm, PE was imaged using a 488 nm argon laser and an emission of 550−625 nm, and Alexa Fluor 488 was imaged using the argon laser with emission spectra of 500−601 nm.

Flow Cytometric Analysis of Nanofactories Targeting Caco-2 Cells. Prior to cytometric analysis, Caco-2 cells were grown to confluence in T-75 flasks. Following a gentle wash with 3 mL of PBS (without $MgCl_2$ or $CaCl_2$), cells were harvested by adding 5 mL of 0.2% EDTA in PBS to the flask and incubating at 37 °C for 15 min. Cells were then resuspended with 5 mL of DMEM + 10% FBS (total volume 10 mL) and spun down at 500*g* for 5 min. Post-centrifugation, cells were resuspended in PBS to a density of approximately 2 million cells/mL. One hundred microliter aliquots were then added to 1.5 mL centrifuge tubes and incubated with 20 μL of labeling solution. Labeling solutions included either PE-labeled CD26 antibody (final concentration 5 μg/mL), Alexa Fluor 647 labeled HGLPT (2 μg/mL), or nanofactories composed of unlabeled CD26 antibody and Alexa Fluor 647 labeled HGLPT. Following 30 min incubation on ice, 1 mL of PBS was added to each tube to dilute unlabeled particles and the tubes were spun for 5 min at 700*g*. The cells were then resuspended in 500 μL of 4% PFA in PBS before analysis. A minimum of 10 000 cells (gated based on forward and side scatter) were counted using a FACS Canto II (BD Biosciences). PE was quantified using a 488 nm solid state laser (585/42 detector), and Alexa Fluor 647 was quantified using a 633 nm HeNe laser (660/20 detector).

***Vibrio harveyi* AI-2 Bioluminescence Assay.** Cell-free culture fluids were tested for the presence of AI-2, capable of inducing luminescence in *V. harveyi* reporter strain BB170. The assays were performed as outlined by Surette and Bassler.[42] Briefly, BB170 was grown for 16 h with shaking at 30 °C in AB medium, diluted 1:5000 in fresh AB medium, and aliquoted (180 μL) to sterile 12 × 75 mm tubes (Fisher Scientific Co., Inc., Pittsburgh, PA) already containing the cell-free culture fluids (20 μL). Negative control tubes contained 20 μL of sterile DMEM no glucose to which 180 μL of diluted BB170 was added. Tubes were shaken at 175 rpm and 30 °C in an air shaker (New Brunswick Scientific), and hourly measurements of luminescence were taken from 3 to 5 h. Luminescence was measured by quantifying light production with a luminometer (EG&G Berthold, Gaithersburg, MD). The AI-2 activities reported were obtained by dividing the RLU produced by the reporter after addition of culture fluid by the RLU of the reporter when growth medium alone was added.[42,54] The obtained values are in a good linear range.

***E. coli* AI-2 Fluorescence Assay.** Cell-free culture fluids were tested for their ability to induce the lsr operon, indicating the presence of AI-2 and a quorum sensing response using the strain MDAI2 (pCT6+pET-GFPuv).[43] Addition of AI-2 to cultures of MDAI2 (pCT6+pET-GFPuv) results in the production of T7 RNA polymerase, which then drives production of GFP. GFP production was quantified using a SpectraMax M2e plate reader (Molecular Devices). Two hundred microliters of each sample was added to a black-walled clear-bottom 96-well culture plate, and exponentially growing (OD 0.4−0.5) MDAI2 (pCT6+pET-GFPuv) cells were added to a final OD of 0.025. These cells were grown at 37 °C in the plate reader for a period of 12 h, over which the cells produce GFP in response to the AI-2 present in the sample. Fluorescence readings were taken every 30 min over this period, and the fluorescence value reported is the difference between the final and beginning fluorescence.

Caco-2 and *E. coli* Co-cultures: Imaging and Flow Cytometry. Cultures of *E. coli* W3110 (pCT6+pET-GFPuv) or MDAI2 (pCT6+pET-GFPuv)[43] were grown overnight at 30 °C and reinoculated the following morning at a 1% inoculum. The cells were then grown at 37 °C to an OD of 0.5 before addition to Caco-2 cell cultures at a final OD of 0.01, unless otherwise noted. Co-cultures were grown at 37 °C in 5% CO_2 for the indicated period of time. Imag-

ing of co-cultures was again conducted with the Leica SP5X using Caco-2 cells grown on glass coverslips within 24-well plates. Following a 15 h co-culture period in PBS, 250 μL was removed from each well (leaving approximately 250 μL) and replaced with 4% PFA in PBS, giving a final concentration of 2% PFA. The co-cultures were then fixed for 15 min at room temperature before the coverslips were removed from the wells and mounted to glass slides using Prolong Gold. Both differential interference contrast (DIC) and GFP images were taken. GFP was imaged using the argon laser at an excitation of 488 nm and emission spectra of 500−550 nm. To prepare *E. coli* samples for flow cytometry, 200 μL of medium was removed from each well and diluted with 300 μL of PBS (without $MgCl_2$ and $CaCl_2$) before addition of 500 μL of 4% PFA (final concentration 2% PFA). The samples were then stored away from light at 4 °C until analysis. A minimum of 20 000 cells were counted using the FACS Canto II. GFP was quantified using the 488 nm solid state laser (530/30 detector).

Acknowledgment. The authors would like to thank A. Beaven (Core Imaging Facility, Cell Biology and Molecular Genetics, University of Maryland) for her assistance with confocal imaging, and T. Dunn (Biomaterials Laboratory, Fischell Department of Bioengineering, University of Maryland) for his help in conducting the flow cytometry studies. This work was also supported by the Defense Threat Reduction Agency (DTRA), the RW Deutsch Foundation, and the National Science Foundation's EFRI program.

Supporting Information Available: Supplemental figures and captions. This material is available free of charge *via* the Internet at http://pubs.acs.org.

REFERENCES AND NOTES

1. Garcia, M. C.; Ray, D. M.; Lackford, B.; Rubino, M.; Olden, K.; Roberts, J. D. Arachidonic Acid Stimulates Cell Adhesion through a Novel P38 Mapk-Rhoa Signaling Pathway That Involves Heat Shock Protein 27. *J. Biol. Chem.* **2009**, *284*, 20936–20945.
2. Quiroga, M. P.; Balakrishnan, K.; Kurtova, A. V.; Sivina, M.; Keating, M. J.; Wierda, W. G.; Gandhi, V.; Burger, J. A. B-Cell Antigen Receptor Signaling Enhances Chronic Lymphocytic Leukemia Cell Migration and Survival: Specific Targeting with a Novel Spleen Tyrosine Kinase Inhibitor, R406. *Blood* **2009**, *114*, 1029–1037.
3. Kerr, J. F. R.; Wyllie, A. H.; Currie, A. R. Apoptosis: A Basic Biological Phenomenon with Wide-Ranging Implications in Tissue Kinetics. *Br. J. Cancer* **1972**, *26*, 239–257.
4. Sundrud, M. S.; Koralov, S. B.; Feuerer, M.; Calado, D. P.; Kozhaya, A. E.; Rhule-Smith, A.; Lefebvre, R. E.; Unutmaz, D.; Mazitschek, R.; Waldner, H.; Whitman, M.; Keller, T.; Rao, A. Halofuginone Inhibits T(H)17 Cell Differentiation by Activating the Amino Acid Starvation Response. *Science* **2009**, *324*, 1334–1338.
5. Lyssiotis, C. A.; Foreman, R. K.; Staerk, J.; Garcia, M.; Mathur, D.; Markoulaki, S.; Hanna, J.; Lairson, L. L.; Charette, B. D.; Bouchez, L. C.; Bollong, M.; Kunick, C.; Brinker, A.; Cho, C. Y.; Schultz, P. G.; Jaenisch, R. Reprogramming of Murine Fibroblasts to Induced Pluripotent Stem Cells with Chemical Complementation of Klf4. *Proc. Natl. Acad. Sci. U.S.A.* **2009**, *106*, 8912–8917.
6. Fuqua, W. C.; Winans, S. C.; Greenberg, E. P. Quorum Sensing in Bacteria—the Luxr−Luxi Family of Cell Density-Responsive Transcriptional Regulators. *J. Bacteriol.* **1994**, *176*, 269–275.
7. Chen, X.; Schauder, S.; Potier, N.; Van Dorsselaer, A.; Pelczer, I.; Bassler, B. L.; Hughson, F. M. Structural Identification of a Bacterial Quorum-Sensing Signal Containing Boron. *Nature* **2002**, *415*, 545–549.
8. Waters, C. M.; Bassler, B. L. The *Vibrio harveyi* Quorum-Sensing System Uses Shared Regulatory Components To Discriminate between Multiple Autoinducers. *Genes Dev.* **2006**, *20*, 2754–67.
9. Higgins, D. A.; Pomianek, M. E.; Kraml, C. M.; Taylor, R. K.; Semmelhack, M. F.; Bassler, B. L. The Major *Vibrio cholerae* Autoinducer and Its Role in Virulence Factor Production. *Nature* **2007**, *450*, 883–886.
10. Le Berre, R.; Nguyen, S.; Nowak, E.; Kipnis, E.; Pierre, M.; Ader, F.; Courcol, R.; Guery, B. P.; Faure, K. Quorum-Sensing Activity and Related Virulence Factor Expression in Clinically Pathogenic Isolates of *Pseudomonas aeruginosa*. *Clin. Microbiol. Infect.* **2008**, *14*, 337–343.
11. Hardie, K. R.; Heurlier, K. Establishing Bacterial Communities by 'Word of Mouth': LuxS and Autoinducer 2 in Biofilm Development. *Nat. Rev. Microbiol.* **2008**, *6*, 635–643.
12. Irie, Y.; Parsek, M. R. Quorum Sensing and Microbial Biofilms. *Curr. Top. Microbiol. Immunol.* **2008**, *322*, 67–84.
13. DeLisa, M. P.; Bentley, W. E. Bacterial Autoinduction: Looking Outside the Cell for New Metabolic Engineering Targets. *Microb. Cell Fact* **2002**, *1*, 5.
14. Williamson, N. R.; Fineran, P. C.; Ogawa, W.; Woodley, L. R.; Salmond, G. P. Integrated Regulation Involving Quorum Sensing, a Two-Component System, a Ggdef/Eal Domain Protein and a Post-Transcriptional Regulator Controls Swarming and Rhla-Dependent Surfactant Biosynthesis in Serratia. *Environ. Microbiol.* **2008**, *10*, 1202–1217.
15. Rasko, D. A.; Moreira, C. G.; Li, D. R.; Reading, N. C.; Ritchie, J. M.; Waldor, M. K.; Williams, N.; Taussig, R.; Wei, S. G.; Roth, M.; Hughes, D. T.; Huntley, J. F.; Fina, M. W.; Falck, J. R.; Sperandio, V. Targeting Qsec Signaling and Virulence for Antibiotic Development. *Science* **2008**, *321*, 1078–1080.
16. Hughes, D. T.; Sperandio, V. Inter-Kingdom Signalling: Communication between Bacteria and Their Hosts. *Nat. Rev. Microbiol.* **2008**, *6*, 111–120.
17. Liu, J.; Meisner, D.; Kwong, E.; Wu, X. Y.; Johnston, M. R. Translymphatic Chemotherapy by Intrapleural Placement of Gelatin Sponge Containing Biodegradable Paclitaxel Colloids Controls Lymphatic Metastasis in Lung Cancer. *Cancer Res.* **2009**, *69*, 1174–1181.
18. Yang, Y.; Bajaj, N.; Xu, P.; Ohn, K.; Tsifansky, M. D.; Yeo, Y. Development of Highly Porous Large Plga Microparticles for Pulmonary Drug Delivery. *Biomaterials* **2009**, *30*, 1947–1953.
19. Tasciotti, E.; Liu, X. W.; Bhavane, R.; Plant, K.; Leonard, A. D.; Price, B. K.; Cheng, M. M. C.; Decuzzi, P.; Tour, J. M.; Robertson, F.; Ferrari, M. Mesoporous Silicon Particles as a Multistage Delivery System for Imaging and Therapeutic Applications. *Nat. Nanotechnol.* **2008**, *3*, 151–157.
20. Liu, Z.; Chen, K.; Davis, C.; Sherlock, S.; Cao, Q. Z.; Chen, X. Y.; Dai, H. J. Drug Delivery with Carbon Nanotubes for *In Vivo* Cancer Treatment. *Cancer Res.* **2008**, *68*, 6652–6660.
21. Murphy, E. A.; Majeti, B. K.; Barnes, L. A.; Makale, M.; Weis, S. M.; Lutu-Fuga, K.; Wrasidlo, W.; Cheresh, D. A. Nanoparticle-Mediated Drug Delivery to Tumor Vasculature Suppresses Metastasis. *Proc. Natl. Acad. Sci. U.S.A.* **2008**, *105*, 9343–9348.
22. Boddapati, S. V.; D'Souza, G. G. M.; Erdogan, S.; Torchilin, V. P.; Weissig, V. Organelle-Targeted Nanocarriers: Specific Delivery of Liposomal Ceramide to Mitochondria Enhances Its Cytotoxicity *In Vitro* and *In Vivo*. *Nano Lett.* **2008**, *8*, 2559–2563.
23. Meers, P.; Neville, M.; Malinin, V.; Scotto, A. W.; Sardaryan, G.; Kurumunda, R.; Mackinson, C.; James, G.; Fisher, S.; Perkins, W. R. Biofilm Penetration, Triggered Release and *In Vivo* Activity of Inhaled Liposomal Amikacin in Chronic *Pseudomonas aeruginosa* Lung Infections. *J. Antimicrob. Chemother.* **2008**, *61*, 859–868.
24. Leduc, P. R.; Wong, M. S.; Ferreira, P. M.; Groff, R. E.; Haslinger, K.; Koonce, M. P.; Lee, W. Y.; Love, J. C.; McCammon, J. A.; Monteiro-Riviere, N. A.; Rotello, V. M.; Rubloff, G. W.; Westervelt, R.; Yoda, M. Towards an *In Vivo* Biologically Inspired Nanofactory. *Nat. Nanotechnol.* **2007**, *2*, 3–7.
25. Fernandes, R.; Roy, V.; Wu, H. C.; Bentley, W. E. Engineered Biological Nanofactories Trigger Quorum Sensing Response in Targeted Bacteria. *Nat. Nanotechnol.* **2009**, *5*, 213–217.

26. Fernandes, R.; Bentley, W. E. AI-2 Biosynthesis Module in a Magnetic Nanofactory Alters Bacterial Response *via* Localized Synthesis and Delivery. *Biotechnol. Bioeng.* **2009**, *102*, 390–399.
27. Lowery, C. A.; Dickerson, T. J.; Janda, K. D. Interspecies and Interkingdom Communication Mediated by Bacterial Quorum Sensing. *Chem. Soc. Rev.* **2008**, *37*, 1337–1346.
28. Vendeville, A.; Winzer, K.; Heurlier, K.; Tang, C. M.; Hardie, K. R. Making 'Sense' of Metabolism: Autoinducer-2, LuxS and Pathogenic Bacteria. *Nat. Rev. Microbiol.* **2005**, *3*, 383–396.
29. Gonzalez Barrios, A. F.; Zuo, R.; Hashimoto, Y.; Yang, Y.; Bentley, W. E.; Wood, T. K. Autoinducer 2 Controls Biofilm Formation in *Escherichia coli* through a Novel Motility Quorum-Sening Regulator (Mqsr, B3022). *J. Bacteriol.* **2006**, *188*, 305–316.
30. Bansal, T.; Englert, D.; Lee, J.; Hegde, M.; Wood, T. K. Differential Effects of Epinephrine, Norephinephrine, and Indole on *Escherichia coli* O157:H7 Chemotaxis Colonization and Gene Expression. *Infect. Immun.* **2007**, *75*, 4597–4607.
31. Bassler, B. L.; Wright, M.; Silverman, M. R. Multiple Signalling Systems Controlling Expression of Luminescence in *Vibrio harveyi*: Sequence and Function of Genes Encoding a Second Sensory Pathway. *Mol. Microbiol.* **1994**, *13*, 273–286.
32. Henke, J. M.; Bassler, B. L. Quorum Sensing Regulates Type III Secretion in *Vibrio harveyi* and *Vibrio parahaemolyticus*. *J. Bacteriol.* **2004**, *187*, 238–248.
33. Rickard, A. H.; Palmer, R. J.; Blehert, D. S.; Campagna, S. R.; Semmelhack, M. F.; Egland, P. G.; Bassler, B. L.; Kolenbrander, P. E. Autoinducer 2: A Concentration-Dependent Signal for Mutualistic Bacterial Biofilm Growth. *Mol. Microbiol.* **2006**, *60*, 1446–1456.
34. Tanaka, T.; Camerini, D.; Seed, B.; Torimoto, Y.; Dang, N. H.; Kameoka, J.; Dahlberg, H. N.; Schlossman, S. F.; Morimoto, C. Cloning and Functional Expression of the T Cell Activation Antigen CD26. *J. Immunol.* **1992**, *149*, 481–486.
35. Rodriguez-Juan, C.; Perez-Blas, M.; Valeri, A. P.; Aguilera, N.; Arnaiz-Villena, A.; Pacheco-Castro, A.; Martin-Villa, J. M. Cell Surface Phenotype and Cytokine Secretion in Caco-2 Cell Cultures: Increased Rantes Production and Il-2 Transcription upon Stimulation with Il-Ib. *Tissue Cell* **2001**, *33*, 570–579.
36. Akerstrom, B.; Brodin, T.; Reis, K.; Bjorck, L.; Protein, G. A Powerful Tool for Binding and Detection of Monoclonal and Polyclonal Antibodies. *J. Immunol.* **1985**, *135*, 2589–2592.
37. Wu, H.; Shi, X.; Tsao, C. Y.; Lewandowski, A. T.; Fernandes, R.; Hung, C.; DeShong, P.; Kobatake, E.; Valdes, J. J.; Payne, G. F.; Bentley, W. E. Biofabrication of Antibodies and Antigens *via* IgG-Binding Domain Engineered with Activatable Pentatyrosine Pro-Tag. *Biotechnol. Bioeng.* **2009**, *103*, 231–240.
38. Schauder, S.; Shokat, K.; Surette, M. G.; Bassler, B. L. The LuxS Family of Bacterial Autoinducers: Biosynthesis of a Novel Quorum-Sensing Signal Molecule. *Mol. Microbiol.* **2001**, *41*, 463–476.
39. Surette, M. G.; Miller, M. B.; Bassler, B. L. Quorum Sensing in *Escherichia coli*, *Salmonella typhimurium*, and *Vibrio harveyi*: A New Family of Genes Responsible for Autoinducer Production. *Proc. Natl. Acad. Sci. U.S.A.* **1999**, *96*, 1639–1644.
40. Miller, C. H.; Duerre, J. A. *S*-Ribosylhomocysteine Cleavage Enzyme from *Escherichia coli*. *J. Biol. Chem.* **1968**, *243*, 92–97.
41. Greene, R. C. Biosynthesis of Methionine. In *Escherichia coli and Salmonella: Cellular and Molecular Biology*; Neidhardt, F., Ed.; American Society for Microbiology Press: Washington, D.C., 1996; Vol. 1, pp 545−560.
42. Surette, M. G.; Bassler, B. L. Quorum Sensing in *Escherichia coli* and *Salmonella typhimurium*. *Proc. Natl. Acad. Sci. U.S.A.* **1998**, *95*, 7046–7050.
43. Shi, X. W.; Tsao, C. Y.; Yang, X. H.; Liu, Y.; Dykstra, P.; Rubloff, G. W.; Ghodssi, R.; Bentley, W. E.; Payne, G. F. Electroaddressing of Cell Populations by Co-Deposition with Calcium Alginate Hydrogels. *Adv. Funct. Mater.* **2009**, *19*, 2074–2080.
44. DeLisa, M. P.; Wu, C. F.; Wang, L.; Valdes, J. J.; Bentley, W. E. DNA Microarray-Based Identification of Genes Controlled by Autoinducer 2-Stimulated Quorum Sensing in *Escherichia coli*. *J. Bacteriol.* **2001**, *183*, 5239–5247.
45. Wang, L.; Hashimoto, Y.; Tsao, C. Y.; Valdes, J. J.; Bentley, W. E. Cyclic Amp (Camp) and Camp Receptor Protein Influence Both Synthesis and Uptake of Extracellular Autoinducer 2 in *Escherichia coli*. *J. Bacteriol.* **2005**, *187*, 2066–2076.
46. Duan, F. P.; March, J. C. Interrupting *Vibrio cholerae* Infection of Human Epithelial Cells with Engineered Commensal Bacterial Signaling. *Biotechnol. Bioeng.* **2008**, *101*, 128–134.
47. Duan, F. P.; Curtis, K. L.; March, J. C. Secretion of Insulinotropic Proteins by Commensal Bacteria: Rewiring the Gut To Treat Diabetes. *Appl. Environ. Microbiol.* **2008**, *74*, 7437–7438.
48. Duan, F. P.; March, J. C. Engineered Bacterial Communication Prevents *Vibrio cholerae* Virulence in an Infant Mouse Model. *Proc. Natl. Acad. Sci. U.S.A.* **2010**, *107*, 11260–11264.
49. Sperandio, V.; Torres, A. G.; Jarvis, B.; Nataro, J. P.; Kaper, B. Bacteria−Host Communication: The Language of Hormones. *Proc. Natl. Acad. Sci. U.S.A.* **2003**, *100*, 8951–8956.
50. Berg, R. D. The Indigenous Gastrointestinal Microflora. *Trends Microbiol.* **1996**, *4*, 430–435.
51. Clarke, M. B.; Sperandio, V. Events at the Host-Microbial Interface of the Gastrointestinal Tract III. Cell-to-Cell Signaling among Microbial Flora, Host, and Pathogens: There Is a Whole Lot of Talking Going On. *Am. J. Physiol.* **2005**, *288*, G1105–G1109.
52. Jayaraman, A.; Wood, T. K. Bacterial Quorum Sensing: Signals, Circuits, and Implications for Biofilms and Disease. *Annu. Rev. Biomed. Eng.* **2008**, *10*, 145–167.
53. Collier-Hyams, L. S.; Neish, A. S. Innate Immune Relationship between Commensal Flora and the Mammalian Intestinal Epithelium. *Cell. Mol. Life Sci.* **2005**, *62*, 1339–1348.
54. Surette, M. G.; Bassler, B. L. Regulation of Autoinducer Production in *Salmonella typhimurium*. *Mol. Microbiol.* **1999**, *31*, 585–595.